Hindawi
Advances in Civil Engineering
Volume 2022, Article ID 2742360, 13 pages
https://doi.org/10.1155/2022/2742360

Research Article

Influence of Load Test Scale on Prediction of Ultimate Bearing Capacity of Aggregate Pier Reinforced Clay

Sung-Ha Baek[1] **and Taeho Bong**[2]

[1]*School of Civil & Environmental Engineering, Hankyong National University, Anseong-si 17579, Republic of Korea*
[2]*Department of Forest Science, Chungbuk National University, Cheongju-si 28644, Republic of Korea*

Correspondence should be addressed to Taeho Bong; thbong@cbnu.ac.kr

Received 22 August 2022; Revised 26 November 2022; Accepted 2 December 2022; Published 16 December 2022

Academic Editor: Xinyu Ye

Copyright © 2022 Sung-Ha Baek and Taeho Bong. This is an open access article distributed under the Creative Commons Attribution License, which permits unrestricted use, distribution, and reproduction in any medium, provided the original work is properly cited.

Predicting the bearing capacity of spread footings on aggregate pier-reinforced soil is particularly important for ground improvement. Various methods for predicting the bearing capacity of spread footings supported on aggregate pier-reinforced clay have been proposed. In addition, many fields or laboratory load tests have been conducted to identify the improvement effects of aggregate pier. However, no study has quantitatively compared the effect of the experimental scale on the prediction of bearing capacity. In this study, multiple linear regression analyses were performed for field and laboratory load tests, and the effects of the load test scale on bearing capacity prediction were identified. The sensitivity analysis showed that the prediction model for the laboratory load test (MLR_L) exhibited a higher sensitivity for the undrained shear strength than that of the field load test model (MLR_F). However, the sensitivity of the area replacement ratio of MLR_L was less than half that of the MLR_F. As the undrained shear strength increased, the predicted bearing capacity of the MLR_L was larger than that of the MLR_F owing to the influence of boundary conditions on the experimental equipment.

1. Introduction

It is widely known that soft soils exhibit problematic properties for construction, such as low shear strength and high compressibility. These engineering properties of soft soils should be improved such that the soil can safely carry structural loads. Aggregate piers are a reinforcement technique used to improve soft soils. They have been increasingly used to reduce settlement and lateral displacement and increase the bearing capacity and stiffness of soil [1–3]. Moreover, aggregate piers function as drains and rapidly dissipate excess pore pressure while accelerating the consolidation of the surrounding soft clay. An important aspect of improved soils is predicting the ultimate bearing capacity according to improvement conditions [4]. Generally, field or laboratory load test results are used to identify the improvement effects of aggregate piers and verify the proposed model for predicting the bearing capacity. Field load tests provide more realistic results than laboratory load tests; however, it is difficult to consider a range of construction conditions in terms of time and money. Additionally, it is difficult to adjust the independent variables that affect bearing capacity in the field. Therefore, an analysis of the improvement effects (such as the bearing capacity and settlement) according to the installation conditions of the aggregate piers was conducted via a laboratory load test. However, most laboratory load tests are performed with small-scale physical models under normal gravity (1 g); therefore, laboratory load tests have the problem of scale effects, as modeling size is reduced considerably compared to the actual size. Another factor influencing experimental results is the boundary effect of the experimental equipment. For these reasons, the engineering characteristics of aggregate piers identified in the laboratory may differ from those in the field. This means that the improvement effects of aggregate piers according to various installation conditions can be confirmed through laboratory load test results; however, there is a limit to its application in the field.

Nevertheless, many researchers have performed laboratory load tests because the improvement effects can be effectively identified. Moreover, laboratory load test results are often used as verification data for numerical analysis [5]. Predictive models for predicting the bearing capacity of aggregate pier-reinforced soil are constantly being proposed and updated using field and laboratory load test results. Most of these studies aim to improve prediction accuracy by using various modeling techniques. However, predictive models for field and laboratory load tests are incompatible. In other words, if the predictive model derived from the laboratory load test is applied to field conditions or vice versa, the prediction error is exceptionally large and unacceptable. However, no studies have identified the relationship between field and laboratory load tests or quantitatively analyzed the improvement effects of aggregate pier installation in an experimental scale.

In this study, field and laboratory load test data for aggregate piers were collected, and the effects of the experimental scale on the prediction of the ultimate bearing capacity of aggregate piers were comparatively analyzed. A total of 85 laboratory load test data were collected from various previous studies, and 76 load test data (in which outliers were removed) were adopted for analysis. For the field load test, a total of 37 data that collected by Stuedlein and Hotlz [3] and updated by Bong et al. [6] were adopted. The ultimate bearing capacity can be obtained from the load-settlement curve, and it varies depending on the calculation method used for it. Therefore, all load-settlement curves in the literature were digitized and redrawn, and the ultimate bearing capacity was determined by using the hyperbolic method. Prediction models for the bearing capacity were established through multiple linear regression (MLR) analysis considering several types of input variables based on the load test data. Two modeling approaches were considered in this study. The first approach involved creating an MLR model using both field and laboratory load test data, ignoring load test scale effects; the second approach involved creating separate MLR models for the field and laboratory load test data, with the same input variables that minimize the mean absolute error (MAE). Here, the optimal input variables were selected based on the results of the leave-one-out cross-validation, and a final MLR model was proposed using all load test data. A sensitivity analysis for the proposed MLR models was performed to identify the differences in the influence of the pier installation conditions on the ultimate bearing capacity according to the experimental scale. In addition, the extent to which the variables affected the differences in bearing capacity was assessed. Finally, a parametric analysis was performed to investigate the difference in effect of increasing the ultimate bearing capacity according to the change in the improvement conditions, and the differences between the field and laboratory load tests were compared.

2. Theoretical Background

2.1. Bearing Capacity of Aggregate Piers. Under a vertical load, aggregate piers transmit the load to the surrounding soil via side friction or lateral confinement [7]. The light vertical load acting on the pier is primarily supported by side friction, and shear stresses are mobilized along the upper part of the pile-soil interface as the applied vertical load increases [8]. The displacement occurs as the load acts on the pier, and the pier system fails after experiencing the maximum support load. Typically, only extremely small relative displacements are required for the bearing capacity to reach the ultimate state [9]. Barkdale and Bachus [10] suggested three failure mechanisms for homogeneous soft soils reinforced with aggregate piers. They noticed that the failure mode differed depending on the pier support condition (floating and end-bearing), and the soil and pier shape conditions (Figure 1).

Bulging failure occurs when the pier length is longer than the critical length, and bulging occurs at depths of 2-3 times the pier diameter, as shown in Figure 1(a). Shear failure generally occurs in short piers supported by firm-bearing strata or when the pier is not considerably stronger than the surrounding matrix soil. The shear failure mechanism is similar to shallow foundation failure, as shown in Figure 1(b). Floating aggregate piers with slenderness ratios of less than three fail owing to plunging, as illustrated in Figure 1(c). Various prediction models have been proposed to predict the ultimate bearing capacity in accordance with the failure modes, which were summarized by Aboshi and Suematsu [11] and Kim and Lee [12].

2.2. Calculation Method for Determining Ultimate Bearing Capacity. The ultimate bearing capacity can be obtained from the load-settlement curve, which is the result of the load test. In the load test, determining the ultimate bearing capacity at which the load-settlement curve reaches almost equilibrium on the settlement axis is often limited owing to various conditions, such as the performance of the test equipment, soil, and test conditions. In addition, the load test was completed without sufficient displacement, leading to failure. Therefore, various interpretation methods have been proposed to determine the ultimate bearing capacity from the load-settlement curve (Figure 2). However, there is still no specific procedure for determining the ultimate bearing capacity of piers.

In tangent intersection method, the stress at the intersection of the initial and final tangent slopes of the load-settlement curve is determined to be the ultimate bearing capacity [13]. The log-log method was used to plot the stress and corresponding settlement on a logarithmic scale, creating two distinct straight lines. Here, the stress at the intersection of the two straight lines was determined to be the ultimate bearing capacity [14]. In the 0.1 B method, the stress that produces a relative settlement of 10% of the width ($s/B = 0.1$) is defined as the ultimate bearing capacity [15]. Duncan and Chang [16] introduced a hyperbolic stress-strain model for soil and used it to determine the primary consolidation settlement and the ultimate bearing capacity [17–21]. In the load-settlement curve, the hyperbolic model is expressed as follows:

$$\frac{s}{q} = a + bs, \tag{1}$$

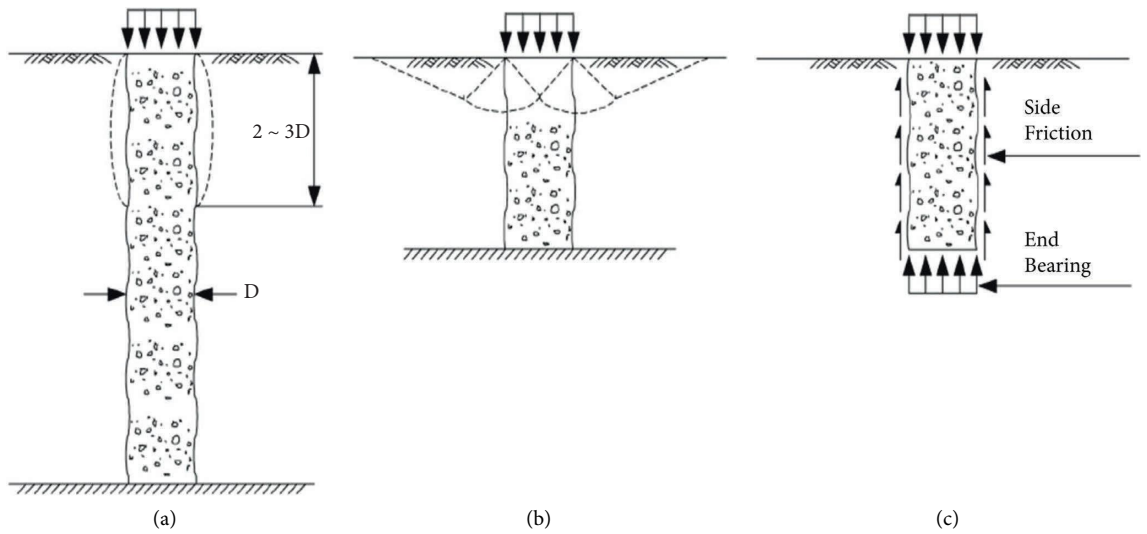

Figure 1: Failure modes of individual columns: (a) bulging failure, (b) shear failure, and (c) punching failure.

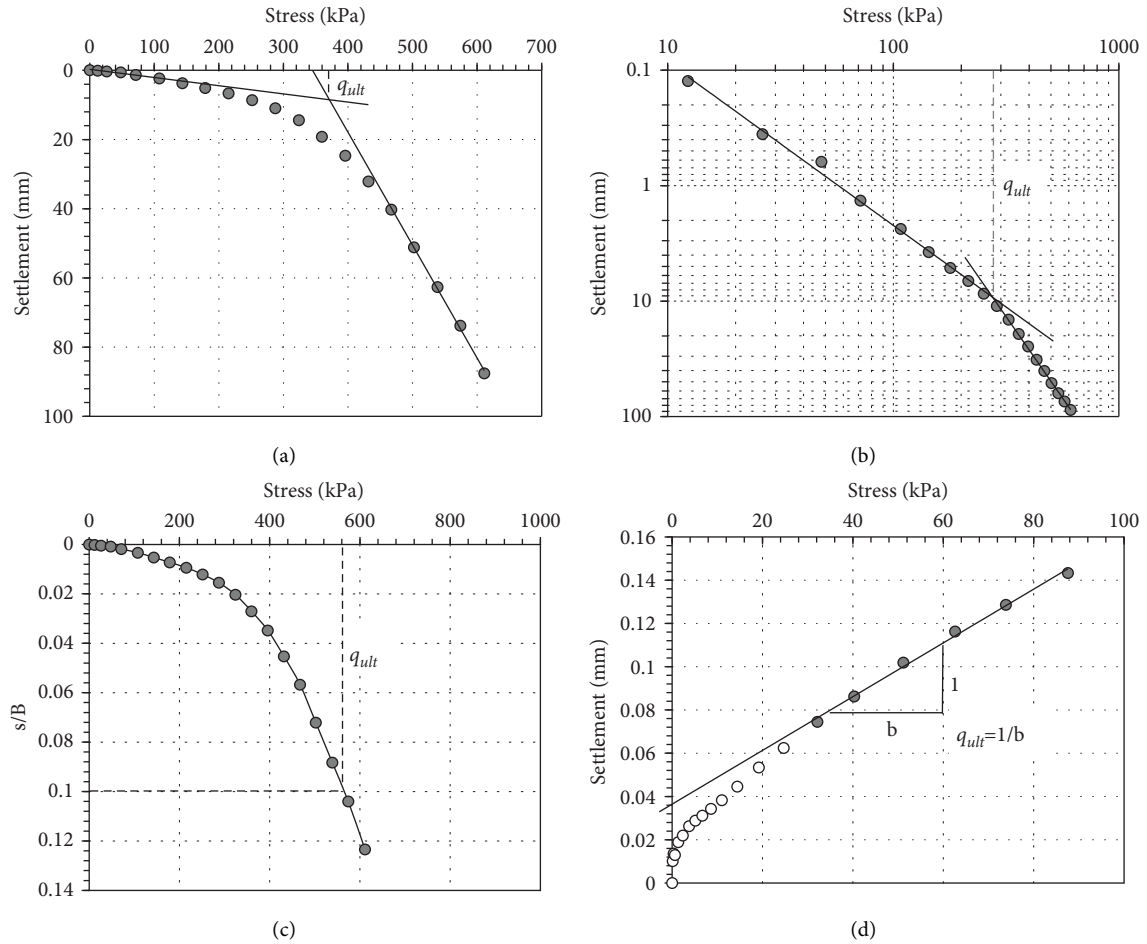

Figure 2: Methods for determining ultimate bearing capacity from load test results: (a) tan tangent intersection method, (b) log-log method, (c) 0.1 B method, and (d) hyperbolic method.

where s is the settlement, q is the stress acting on the foundation, and a and b are linear regression constants. The inverse slope of this linear relationship ($1/b$) is defined as the ultimate bearing capacity.

Lutenegger and Adams [22] compared the difference in ultimate bearing capacity according to the four interpretation methods as shown in Figure 2, and the largest ultimate bearing capacity was generally determined in the order of the hyperbolic, 0.1 B, tangent intersection, and log-log methods, respectively. Determining the ultimate bearing capacity in a consistent manner is significantly important because even the same load test results can lead to quite different results depending on the method of determining the ultimate bearing capacity. The ultimate bearing capacity provided in the literature was defined using various methods; however, some studies did not provide it. Unfortunately, it is impossible to obtain raw data for the load-settlement curves provided in numerous studies. Therefore, in this study, all load-settlement curves in the literature were digitized and redrawn, and the ultimate bearing capacity was determined using the hyperbolic method.

2.3. Prediction of Ultimate Bearing Capacity. Since the 1970s, various methodologies have been developed to predict the bearing capacity of reinforced soil based on analytical methods [23–26], empirical methods [1, 27, 28], and numerical methods [10, 29–31]. However, despite these studies, the existing models exhibit large errors and a high degree of prediction variability; therefore, they are unsuitable for practical use [3]. Stuedlein and Holtz [3] proposed new models that modify the methods proposed by Hughes et al. [24] and Mitchell [28]. This resulted in improved prediction accuracy and reduced variability. Later, Bong et al. [6] modified these models to consider the effect of the area-replacement ratio more reasonably. Recently, artificial intelligence (AI) has been used to solve complex geotechnical problems. Specifically, artificial neural networks (ANN) and deep neural networks (DNN) have been used to predict the bearing capacity of aggregate pier-reinforced soils [1, 32, 33]. Bong et al. [1] proposed an MLR and DNN models for predicting the ultimate bearing capacity using the same 37 field-load test data used in this study. They proposed MLR modeling considering nonlinearity with dependent variables by adding various variable forms, such as x^2, $1/x$, $\ln(x)$, and $\sqrt{x}$. As a result, both models were able to significantly improve the prediction accuracy compared to the existing models, and the MLR and DNN models were found to have similar accuracies for the ultimate bearing capacity prediction. Using the load test data generated by Bong et al. [1], Dadhich et al. [34] also performed modeling to predict the ultimate bearing capacity of aggregate pier-reinforced clay using machine learning. Although artificial intelligence models, such as ANN and DNN, have achieved success in improving prediction accuracy, these black-box models have limitations in identifying the relationship between independent and dependent variables. This study aims to identify the effects of the load test scale on the prediction of the bearing capacity, rather than improving the prediction accuracy. Therefore, an MLR model that could clearly identify the relationship between the independent and dependent variables was adopted. In particular, the MLR modeling method proposed by Bong et al. [1] has demonstrated high performance in predicting the ultimate bearing capacity of aggregate pier-reinforced clay and showed high prediction accuracy compared to the DNN model.

2.4. Multiple Regression Analysis. MLR is a widely used statistical technique to model the linear relationship between a dependent variable and two or more independent variables and can be expressed as follows:

$$y = \beta_0 + \beta_1 x_1 + \beta_2 x_2 + \cdots + \beta_n x_n + \varepsilon, \tag{2}$$

where x_i is the independent variable, β_0 is a constant (y-intercept), and ε is an error term. β_0, β_1, …, β_n are the regression coefficients representing the change in y according to the change in x. Equation (2) can be expressed using a matrix form, and the regression coefficients of MLR can be estimated using the least squares method as follows:

$$[\beta] = \left([X]^T [X]\right)^{-1} [X]^T [Y], \tag{3}$$

where $[X]$ is the matrix for independent variables, $[\beta]$ is the matrix of regression coefficients, and $[Y]$ is the matrix for dependent variables. Although various independent variables and their combinations can be considered in MLR modeling, the MLR model is too complex to account for all possible independent variables. In particular, some independent variables may not have a substantial effect on the outcomes or reduce accuracy. Therefore, appropriate input variables must be selected to establish an optimal MLR model. Commonly used independent variable selection methods include forward selection, backward elimination, and the stepwise method. However, these methods do not always guarantee an optimal variable selection. When various equation forms are considered for variables such as x and x^2, other input variables can be selected because of multicollinearity, even though x and x^2 are the optimal variables considering nonlinearity. Helsel and Hirsch [35] discussed the disadvantages of existing variable selection methods. By evaluating all combinations of input variables, they noted that there were numerous benefits to selecting the optimal input variables. Therefore, MLR modeling was performed in the same manner as suggested by Bong et al. [1], selecting the optimal model by considering various equation forms of input variables and their combinations. Figure 3 presents a process diagram of the MLR model suggested by Bong et al. [1].

For convenience of application, the number of input variables was set to four because there was no significant difference in accuracy when using four and five input variables. Two modeling approaches were considered to estimate the ultimate bearing capacity using field and laboratory load test data:

(i) Approach 1: MLR for the ultimate bearing capacity was performed using all the load test data without distinguishing between the field and laboratory load tests

(ii) Approach 2: MLRs using the same input variables were performed for field and laboratory load tests, respectively

Although the influence of the input variables on the ultimate bearing capacity is different between the field and laboratory load tests, Approach 1 ignores the experimental scale effect and builds an MLR model using both field and laboratory load test data. This approach is simple and can be applied universally without distinguishing between the field and the laboratory load tests. Approach 2 involved performing each MLR by considering the scale effect of the load test. It is important to note that although MLR modeling for the field and laboratory load tests was performed, the MLR models were created to have the same input variables. If optimal MLR models are selected using only the minimum prediction error, the input variables of the MLR models for the field and laboratory load tests may be different, and the difference between them would be difficult to compare quantitatively. Therefore, the two MLR models were established to have the same input variables, while having the lowest MAE.

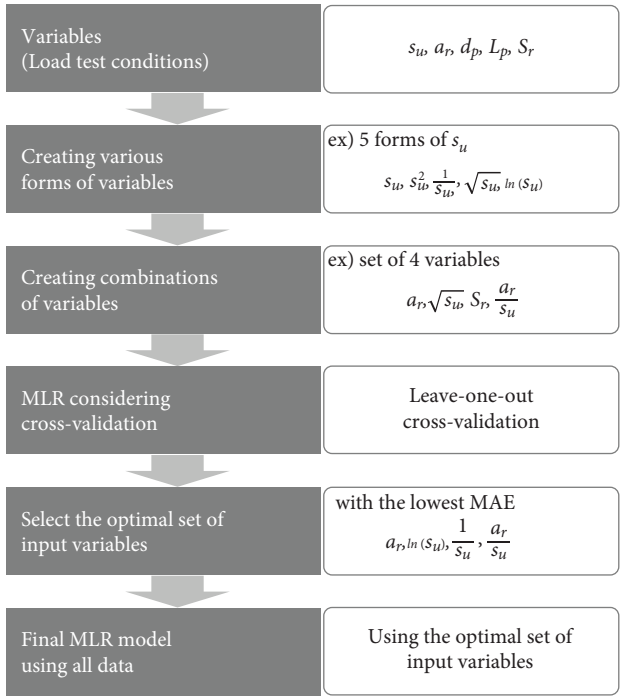

Figure 3: Diagram of MLR modeling process.

3. Results and Discussion

3.1. Load Test Database. Laboratory load test data were collected from various studies, and the following criteria were considered to ensure the quality of data: (a) the load test results that provide accurate information on the experimental conditions with the load-settlement curve in the literature, (b) load test performed on homogeneous soil, and (c) the width of the experimental equipment more than twice the loading plate. The pier supporting conditions were divided into floating and end-bearing conditions, and the bearing capacity could be large when the end-bearing pier had a small slenderness ratio (S_r). Bulging failure can occur at shallow depths of less than 2–3 times the pier diameter [10, 36]. Therefore, for the end-bearing condition, only the case of $S_r \geq 4$ was adopted, and the effect of the pier supporting condition was excluded in this study. Thus, 85 laboratory load test data were collected. However, these load tests have been conducted by various researchers, and the results could have been influenced by many factors, including experimental error, soil type, and equipment. Hence, some load tests may yield unusual results that can function as a major factor in distorting the model. Consequently, data preprocessing is required to identify and remove outliers. Bong et al. [6] found and removed load test data that reduced model accuracy by investigating the overall absolute error change due to the removal of a load test. To remove outlier data for laboratory load tests, the optimal MLR model with the lowest MAE was selected using all the laboratory load test data. Subsequently, the change in the MAE according to the removal of each load test was investigated. The results are shown in Figure 4.

The dotted line indicates the MAE (equal to approximately 60.3 kPa) when all the loading test data were used for the MLR model. It was found that if some load tests were excluded, the overall MAE was reduced considerably.

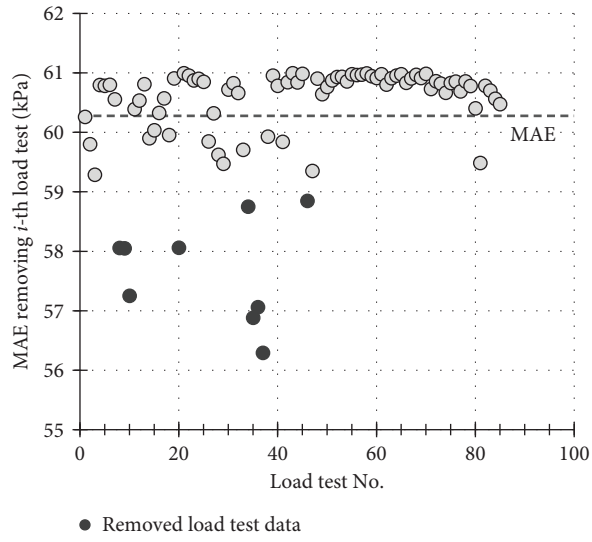

Figure 4: MAE change due to the removal of each load test.

Therefore, nine load tests corresponding to approximately 10% of the total data were excluded from the MLR model. The ranges of the field and laboratory loading test conditions are summarized in Table 1, and the box plots for the undrained shear strength (s_u), area replacement ratio (a_r), S_r, and ultimate bearing capacity (q_{ult}) are compared in Figure 5.

The s_u reproduced in the laboratory was low compared to that of the field, and the average s_u for the field was three times higher than that of the laboratory. In particular, s_u in the field varied broadly, from 12 to 100. The range of a_r for the field and laboratory was similar, but the interquartile range (IQR) for the laboratory was relatively low. In other

Table 1: Range of field and laboratory load test conditions.

Load test		s_u (kPa)	a_r (%)	d_p (m)	L_p (m)	S_r	q_{ult} (kPa)
Field	Min	12.0	16.0	0.3	1.5	2.0	177.0
	Max	100.0	122.0	1.0	14.0	26.7	1346.0
	Mean	47.1	72.4	0.7	5.1	8.3	745.7
	COV (%)	43.1	46.9	22.1	64.6	89.0	43.6
Laboratory	Min	5.0	4.0	0.02	0.1	3.0	53.5
	Max	35.0	100.0	0.10	0.6	16.0	1087.1
	Mean	14.7	35.6	0.05	0.3	6.7	299.4
	COV (%)	65.1	95.0	42.05	31.7	35.9	97.0

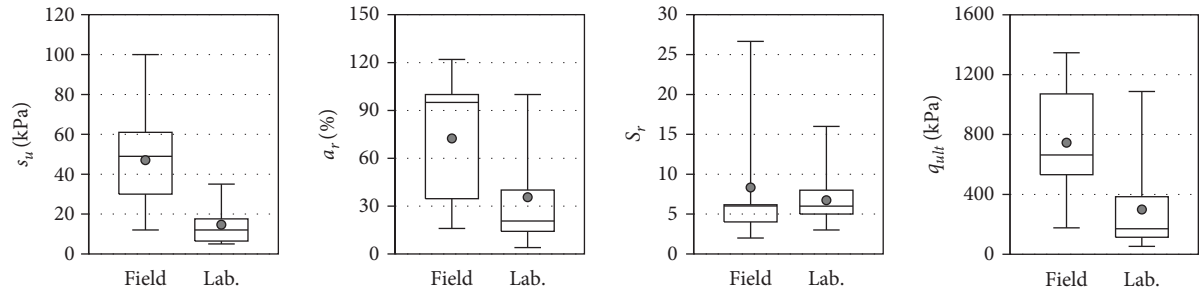

Figure 5: Comparison of box plot for field and laboratory test conditions.

words, most of the laboratory loading tests were performed under a low a_r. The average S_r of the field was higher with a wider range than that of the laboratory because the specific test was performed with a high S_r of 26.7. However, the IQR for the laboratory was slightly higher than that for the field. The range of q_{ult} was relatively similar, but the IQR for the laboratory was lower than that for the field because the majority of the laboratory load tests had a low q_{ult}.

3.2. Estimation of Ultimate Bearing Capacity Using Approach 1. Approach 1 involves establishing an MLR model using all the load test data, comprising a total of 113 load test data, 37 of which were field load tests, and 76 of which were laboratory load tests. The number of input variables was set to four, and various equation forms of input variables and their combinations were considered as the input variables of the MLR. In this study, the diameter and length of the pier, which are variables related to the pier shape, were not considered directly because of the differences in scale between the field and laboratory. Therefore, the effect of the pier shape was only considered by S_r. As a result, three variables (s_u, a_r, and S_r) were considered in Approach 1. To consider the nonlinear relationship between the independent and dependent variables in MLR, several types of input values were generated, given frequently used parameter types, as summarized in Table 2.

Consequently, 5,985 MLR models were generated by considering combinations of 21 input variable types ($_{21}C_4 = 5{,}985$). Leave-one-out cross-validation was performed to evaluate the prediction error of the independent loading test, and the top three MLR models that showed the best performance based on mean absolute error (MAE) were selected. The results are summarized in Table 3.

Although the combination of ($\sqrt{s_u a_r}$, S_r, $\sqrt{S_r}$, $\sqrt{s_u} S_r$) provided the lowest MAE, the difference was only 0.2 kPa from the combination of (a_r, ln (s_u), $1/s_u$, a_r/s_u), which showed the second-lowest MAE. However, compared with those of the first-ranked model, the bias of the second-ranked model was slightly lower; its variability was approximately 8% lower, indicating that a more robust prediction was possible considering the entire bearing capacity range. Therefore, the final MLR model was established using all the load test data and a combination of input variables for the second-ranked model. The best-fitting MLR model is expressed as follows:

$$q_{ult} = 3.44 a_r + 2611.6 \frac{1}{s_u} + 465.7 \ln(s_u) - 14.18 \frac{a_r}{s_u} - 1220.3, \quad (4)$$

where a_r and s_u are measured as percentages and kPa, respectively, and the best MLR model obtained using both field and laboratory data (MLR_T) is expressed as a function of only a_r and s_u. Figure 6 presents a comparison of the observed and predicted ultimate bearing capacities of the final MLR model for Approach 1, and the results are summarized in Table 4.

The MAE, MAPE (mean absolute percentage error), bias, and coefficient of variation (COV) in the bias for MLR_T were 91.7 kPa, 21.99%, 1.01, and 27.2%, respectively. The proposed MLR_T was found to have an error of approximately 20% considering the bearing capacity size, and it showed a relatively high error rate at a low bearing capacity because the MLR coefficients were calculated by considering the minimization of the total error. Although the proposed MLR_T was modeled considering field and laboratory load test data, it showed a relatively low MAE compared with the existing models. However, there were still large prediction errors for

Table 2: Various types of input variables for MLR modeling (Approach 1).

Variable	s_u	a_r	s_u, a_r	Shape factor
Input parameter	s_u, s_u^2, $1/s_u$, $\sqrt{s_u}$, $\ln(s_u)$	a_r, a_r^2, $1/a_r$, $\sqrt{a_r}$, $\ln(a_r)$	$s_u a_r$, $\sqrt{s_u a_r}$, $1/s_u a_r$, s_u/a_r, a_r/s_u	S_r, $1/s_r$, $\sqrt{S_r}$, $\sqrt{1/s}$, $s_u S_r$, $\sqrt{s_u} S_r$

Table 3: Cross-validation error evaluation for input variables (Approach 1).

Rank	Input variables	MAE (kPa)	R^2	Bias, λ	
				Mean	COV (%)
1	$\sqrt{s_u a_r}$, S_r, $\sqrt{S_r}$, $\sqrt{s_u} S_r$	95.3	0.86	1.02	36.3
2	a_r, $\ln(s_u)$, $1/s_u$, a_r/s_u	95.5	0.85	1.01	28.5
3	s_u, $1/s_u$, $s_u a_r$, $\sqrt{s_u}$	96.2	0.85	1.00	28.2

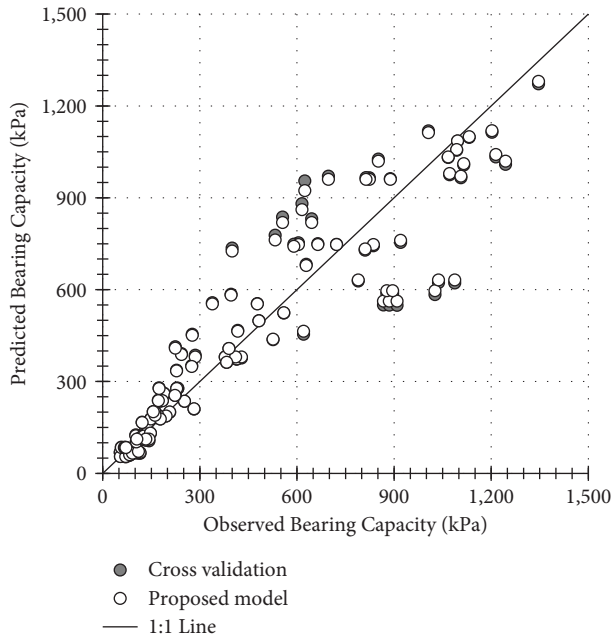

Figure 6: Comparison of observed and predicted ultimate bearing capacity of the proposed MLR model for approach 1.

Table 4: Prediction performance of the proposed model and it cross-validation (approach 1).

Model	Evaluation case	MAE (kPa)	MAPE (%)	R^2	Bias, λ	
					Mean	COV (%)
MLR_T	Cross-validation	95.5	22.91	0.85	1.01	28.5
MLR_T	Proposed model	91.7	21.99	0.86	1.01	27.2

some load test conditions because MLR_T considered only two variables (a_r and s_u), and the scale effects of the laboratory load test were neglected.

3.3. Estimation of Ultimate Bearing Capacity Using Approach 2. Approach 2 involves establishing MLR models for field and laboratory load tests using the same input variables. As in Approach 1, the number of input variables was set to four, and various equation forms of the input variables and their combinations were generated as input variables of the MLR. However, unlike Approach 1, the diameter and length of the pier were also considered as input variables because they were considered for modeling based on the load test scale. Bong et al. [1] proposed an MLR model to predict the ultimate bearing capacity in a field load test, and the depth of the footing embedment was considered as an input variable. However, the depth of the footing embedment was not considered for MLR modeling in this study because its effect on the bearing capacity was small. Moreover, the embedment depth was zero in most of the laboratory load tests. As a result, five variables (s_u, a_r, d_p, L_p, S_r) were considered in Approach 2, and several types of input values were generated, as summarized in Table 5.

Consequently, 17,550 MLR models were generated considering the combinations of 27 input variable types ($_{27}C_4 = 17{,}550$), and leave-one-out cross-validation was performed for each model according to the load test scale.

Table 5: Various types of input variables for MLR modeling in approach 2.

Variable	s_u	a_r	s_u, a_r	Shape factor
Input parameter	s_u, s_u^2, $1/s_u$, $\sqrt{s_u}$, $\ln(s_u)$	a_r, a_r^2, $1/a_r$, $\sqrt{a_r}$, $\ln(a_r)$	$s_u a_r$, $\sqrt{s_u a_r}$, $1/s_u a_r$, s_u/a_r, a_r/s_u	d_p, $1/d_p$, d_p^2, $\sqrt{d_p}$, L_p, $1/l_p$, L_p^2, $\sqrt{L_p}$, S_r, $1/s_r$, $\sqrt{S_r}$, $\sqrt{1/s_r}$

The optimal combination of input variables representing the best performance was selected based on the weighted average of the MAE for the two load test scales, considering the amount of data. The results of the error evaluation for the top three MLR models are summarized in Table 6.

The combination of (s_u^2, $\ln(a_r)$, $\sqrt{s_u a_r}$, $\sqrt{1/s_r}$), which provided the lowest MAE and bias, was selected as the best input variable, and the final MLR models were established using all load test data. The best-fitting MLR models for the field (MLR_F) and laboratory (MLR_L) load tests are expressed in equations (5) and (6), respectively.

Table 6: Cross-validation error evaluation for input variables (approach 2).

Rank	Input variables	MAE (kPa)	R^2	Bias, λ	
				Mean	COV (%)
1	s_u^2, $\ln(a_r)$, $\sqrt{s_u a_r}$, $\sqrt{1/s_r}$	52.2	0.96	1.02	21.1
2	s_u^2, $\ln(a_r)$, $\sqrt{s_u a_r}$, $1/s_r$	52.3	0.96	1.03	21.5
3	s_u^2, $\ln(a_r)$, $\sqrt{s_u a_r}$, $1/L$	52.7	0.96	1.58	371.4

$$\mathrm{MLR_F}: q_{ult} = -0.04 s_u^2 - 264.3 \ln(a_r) + 23.49 \sqrt{s_u a_r} - 517.3 \sqrt{\frac{1}{S_r}} + 841.5, \tag{5}$$

$$\mathrm{MLR_L}: q_{ult} = 0.56 s_u^2 - 10.5 \ln(a_r) + 8.44 \sqrt{s_u a_r} - 289.1 \sqrt{\frac{1}{S_r}} + 112.1. \tag{6}$$

The sign of the regression coefficient indicates whether each independent variable has a positive or negative correlation with the dependent variable. The regression coefficients for both models have the same sign, except s_u^2. However, these values were considerably different. This means that the effect of each independent variable on q_{ult} was different, owing to the scale effects of the load test. Figure 7 presents a comparison of the observed and predicted ultimate bearing capacities of the final MLR models for Approach 2, and the results are summarized in Table 7.

The observed and predicted ultimate bearing capacities were in good agreement, and the weighted average MAE for both MLR models (MLR_F and MLR_L) was 47.2 kPa, which improved the total prediction accuracy by 50% compared with that of Approach 1. The MAE, MAPE, R^2, and bias were 65.4 kPa, 10.51%, 0.93, and 1.02 for MLR_F and 38.3 kPa, 17.89%, 0.96, and 1.02, for MLR_L, respectively. The MAE of the MLR_F was approximately 27 kPa higher than that of MLR_L. However, the ultimate bearing capacity ranges for the field and laboratory load tests differed, as shown in Figure 5. Therefore. The MAPE was calculated to compare the prediction performance on different scales. The predictive performance evaluation based on the MAPE was found to be higher in MLR_F than in MLR_L because some laboratory load tests showed a high error in the low bearing capacity range.

3.4. Sensitivity Analysis. The sensitivity of the input variables may differ depending on the scale of the load test. This can be understood indirectly by comparing the regression coefficients of equations (5) and (6). However, the sensitivity of each input variable cannot be compared because they are expressed in various forms. Therefore, a sensitivity analysis based on Monte Carlo simulations was performed to evaluate and compare the influence of each input variable on q_{ult} according to the load test scale. The range of each input variable was estimated for the field and laboratory load tests, as summarized in Table 1. As demonstrated by Bong et al. [1], S_r can be directly used in a sensitivity analysis instead of considering L_p and d_p. Spearman rank correlations were estimated from the Monte Carlo simulation results, and the tornado diagram is shown in Figure 8.

The tornado diagram shows the influence of the input variables on the ultimate bearing capacity, and both load test scales showed a higher influence in the order of s_u, a_r, and S_r, indicating a positive relationship with the bearing capacity. However, the degree of influence differed according to the load test scale. For the field load test, the influence of s_u was the largest, with a correlation coefficient of 0.72, and a_r was found to be an important variable, with a correlation coefficient of 0.58. On the other hand, compared with the field load test, the influence of s_u was extremely high with a correlation coefficient of 0.96 in the laboratory load test; the influence of a_r was found to be half. The S_r in both MLR models showed low sensitivity, and the differences were not significant.

3.5. Comparison of Improvement Effects. In the existing literature, load tests were performed considering various installation conditions of the pier, and the improvement effects of aggregate pier-reinforced clay were quantitatively

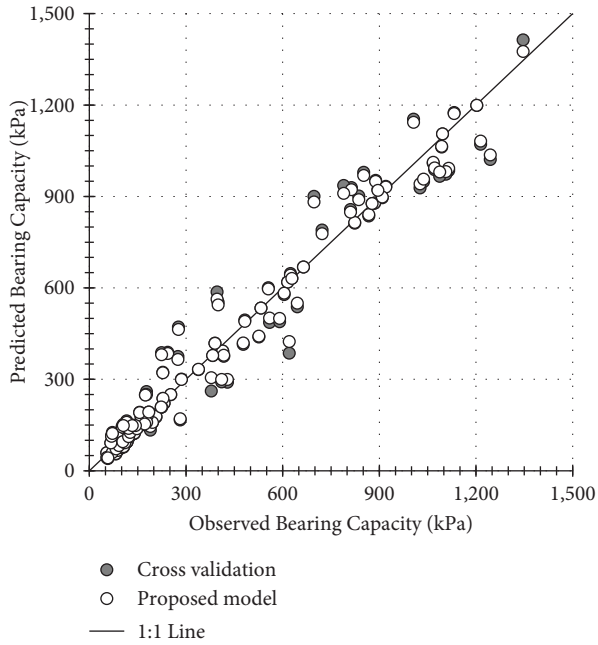

Figure 7: Comparison of observed and predicted ultimate bearing capacity by the proposed MLR models for approach 2.

Table 7: Prediction performance of the proposed model and it cross-validation (approach 2).

Model	Evaluation case	MAE (kPa)	MAPE (%)	R^2	Bias, λ	
					Mean	COV (%)
MLR_F & MLR_L	Cross-validation (field + lab.)	52.2	16.75	0.96	1.02	21.1
MLR_F & MLR_L	Proposed model (field + lab.)	47.2	15.47	0.96	1.02	19.2
MLR_F	Proposed model (field)	65.4	10.51	0.93	1.02	13.7
MLR_L	Proposed model (lab.)	38.3	17.89	0.96	1.02	21.5

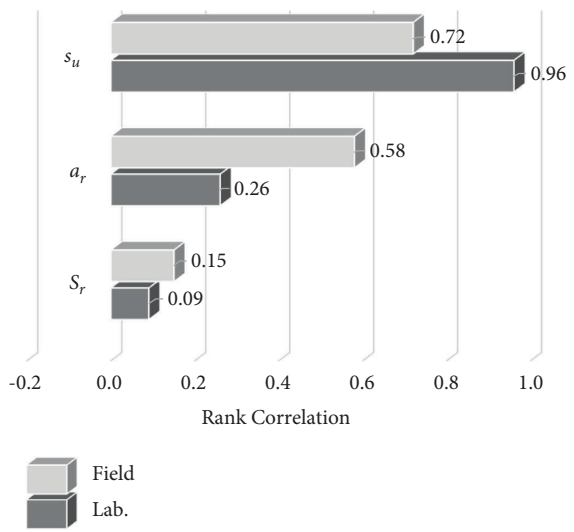

Figure 8: Tornado diagram of relative influence of the input variables on MLR models.

identified based on these results. However, as mentioned earlier, the influence of the input variables depends on the load test scale; thus, the effects of ground improvement are also different. Therefore, the difference in ground improvement effects according to the installation conditions of the pier was analyzed using the proposed MLR models (MLR_F and MLR_L). By considering the range of input variables that fall within the range of both field and laboratory load test data, the range was set to 15–35 kPa for s_u, 20–100% for a_r, and 3–15 for S_r. Five input values with the

same interval for each input variable were considered, and the q_{ult} for a total of 125 cases was calculated. Figure 9 shows a comparison of the ultimate bearing capacity for field and laboratory load tests for 125 cases.

For the same s_u, q_{ult} increased owing to the increase in a_r and S_r; however, the effect of S_r was exceedingly minor compared to that of a_r. Under the same pier installation conditions, the predicted q_{ult} values of the two MLR models were relatively similar at s_u lower than 20 kPa, regardless of a_r or S_r. However, the difference was larger as s_u increased. In particular, the average q_{ult} for the laboratory load test scale at $s_u = 35$ kPa was 1.69 times larger than that of the field load test scale. The difference in q_{ult} according to the load test scale can be calculated as the difference between the two MLR models, as shown in equation.

$$\mathrm{MLR_L} - \mathrm{MLR_F}: \; q_{ult} = 0.60 s_u^2 + 253.8 \ln(a_r) - 15.1\sqrt{s_u a_r} + 228.2\sqrt{\frac{1}{S_r}} - 729.4. \quad (7)$$

Sensitivity analysis was performed using equation (7) to assess the extent to which the variables were affected the difference in q_{ult} between the field and laboratory load tests. Here, the data range was set as the range to which both field and laboratory load test data simultaneously belong. The tornado diagram for Spearman rank correlations is shown in Figure 10.

It was found that s_u had a dominant effect on the difference in q_{ult} according to the load test scale, and the influence of s_u in predicting the bearing capacity was overestimated at the laboratory load test scale. The Spearman rank correlation coefficient of a_r and S_r showed negative values because, as shown in Figure 8; the correlation coefficient of the two variables for the field load test was lower than that in the laboratory load test.

Figure 11 shows the average difference in q_{ult} according to the range of s_u when the other pier installation conditions are the same. The difference in q_{ult} according to the load test scale increases as s_u increases owing to scale effects and the influence of the boundary constraint caused by the experimental equipment. Under laboratory load test conditions, the soil mass with the installed aggregate pier was constrained by a rigid wall. If the boundary condition was within the range in which the horizontal stress was transmitted by the loaded spread footing, it acted as a factor that increased the confining pressure acting on the pier. Additionally, although the pier support condition only considered floating and end-bearing conditions with S_r of 4 or more, the insufficient height of the experimental equipment affected the bearing capacity. The increase in q_{ult} with increasing s_u and

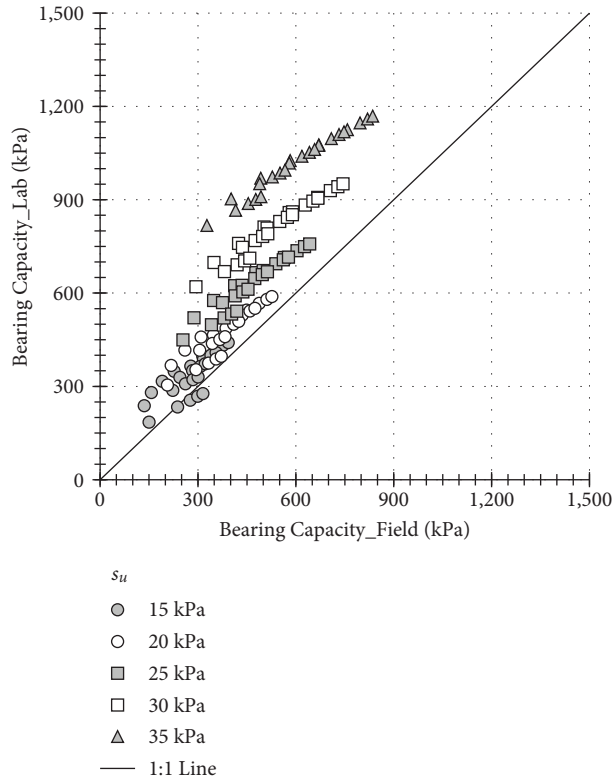

Figure 9: Comparison of observed and predicted ultimate bearing capacity of the proposed MLR models for approach 2.

a_r was investigated using the proposed MLR models. The S_r was fixed at 9, which is the median value of the range, as its effect on q_{ult} was the smallest (Figure 12).

Figure 12(a) shows the change in q_{ult} according to a_r for various values of s_u applied from 15 to 35 kPa, in order from bottom to top. At the field load test scale, the increase rate of q_{ult} with increasing a_r was small at a low s_u. However, this increased as s_u increased, whereas the change in q_{ult} according to a_r was almost similar regardless of s_u at the laboratory load test scale. Figure 12(b) shows the change in q_{ult} according to s_u for various values of a_r applied from 20% to 100%, in order from bottom to top. At the laboratory load test scale, the increase rate of q_{ult} according to s_u was almost similar regardless of a_r, and the increase in q_{ult} with increasing s_u was notable. At the field load test scale, q_{ult} also increased with increasing s_u, and this was more pronounced when a_r was high. However, compared to the laboratory load test scale, the rate of increase of q_{ult} with increasing s_u was found to be lower. The linear slope of the laboratory load test scale was 3.6 times greater at $a_r = 20\%$ and 1.6 times greater at $a_r = 100\%$ than that of the field load test scale.

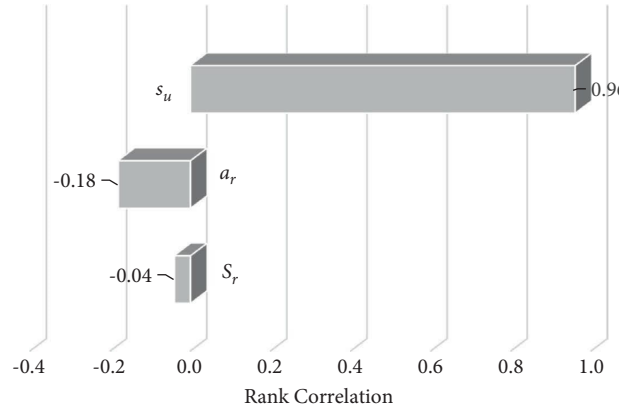

Figure 10: Tornado diagram of relative influence of the input variables on differences between MLR models (MLR_L-MLR_F).

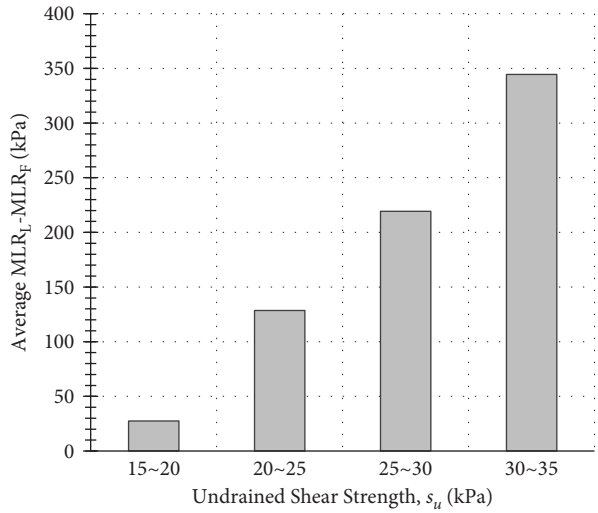

Figure 11: Difference in bearing capacity according to the load test scales.

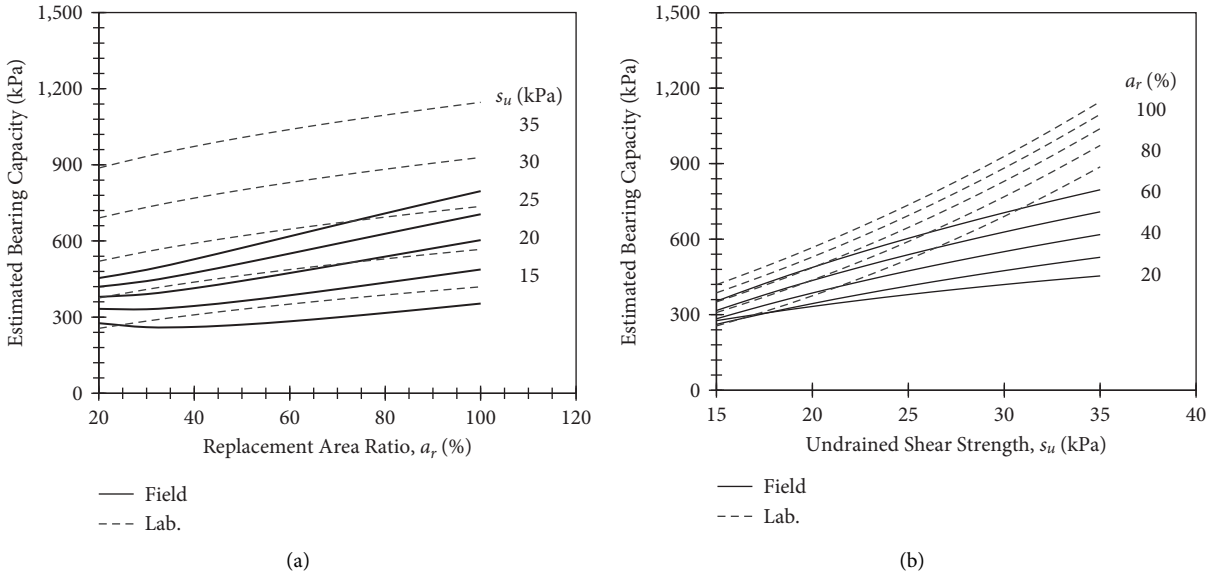

Figure 12: Change in ultimate bearing capacity of aggregate pier-reinforced clay according to (a) a_r and (b) s_u.

4. Conclusions

Compared to expensive field load tests, laboratory load tests are economical, and the independent variables are easier to control. However, laboratory load tests are usually performed on a small scale and suffer from scale effects. Therefore, the effects of the improvement conditions on the bearing capacity are different from those at the field. In this study, the effects of the improvement conditions for predicting the bearing capacity according to the load test scale were quantitatively analyzed and compared. Based on the results of this study, the following conclusions were drawn:

(1) 85 laboratory load test data that satisfied certain criteria were collected from the literature. All load-settlement curves in the literature were digitized and redrawn, and the ultimate bearing capacity was determined using the hyperbolic method. Then, 75 laboratory load tests were selected by finding outliers that reduce prediction performance using leave-one-out cross-validation and excluding them from modeling.

(2) Two modeling approaches were used to predict the bearing capacity. Approach 1 was used to model the entire data set without considering the experimental scale, whereas Approach 2 was used to model each load test scale while using the same input variable.

(3) In Approach 1, the final MLR model that showed the best performance was the prediction model only by s_u and a_r with MAE = 91.7 kPa and MAPE = 21.99%, which is relatively insignificant compared to the existing models. However, there are still large prediction errors that are difficult to apply in practice.

(4) In Approach 2, the combination of $(s_u^2, \ln(a_r), \sqrt{s_u a_r}, \sqrt{1/S_r})$ was selected as the best input variable in the two MLR models with an average MAE of 47.2 kPa. The MAE, MAPE, R^2, and bias were 65.4 kPa, 10.51%, 0.93, and 1.02 for MLR_F and 38.3 kPa, 17.89%, 0.96, and 1.02, for MLR_L, respectively. Therefore, effective prediction of the ultimate bearing capacity was possible using the proposed MLR models, resulting in improved prediction accuracy.

(5) Sensitivity analysis showed that s_u in MLR_L had a higher sensitivity with a correlation coefficient of 0.96 compared to MLR_F. In contrast, the sensitivity of a_r in MLR_L was less than half that of MLR_F. The S_r in both MLR models had low sensitivity, and the difference between the two MLR models was not significant.

(6) The difference in the bearing capacity prediction according to the experimental scale was expressed as an equation, and s_u with a correlation coefficient of 0.96 was found to have the greatest effect on the difference in bearing capacity.

(7) Under the same improvement conditions, the predicted q_{ult} of MLR_L and MLR_F were relatively similar at s_u lower than 20 kPa. However, the difference in q_{ult} according to the experimental scale was found to be considerably larger with increasing s_u, and the average q_{ult} for the laboratory scale at $s_u = 35$ kPa was 1.69 times larger than that at the field scale because of the scale effects and influence of boundary conditions on the experimental equipment in the laboratory load test.

The influence of the experimental scale on the bearing capacity differs depending on the experimental conditions (e.g., scaling factor and boundary condition). However, there is a limit to separately identifying these effects using the collected load test data. The proposed MLR models can effectively predict the bearing capacity with high prediction accuracy using only three variables (s_u, a_r, S_r) and grasp the influence of the load test scale and the difference in ultimate bearing capacity. Moreover, the MLR models can be easily improved by updating the coefficients by considering the addition of new load test data. However, the proposed MLR models are regression equations based on a load-test database. Therefore, it is necessary to check whether the range of the input data is included in the load test database summarized in Table 1, and caution should be exercised when applying the proposed MLR models to new input data that lie outside the bounds of the load test database.

Data Availability

The data used to support the findings of this study are provided as supplementary data.

Conflicts of Interest

The authors declare that they have no conflicts of interest.

Acknowledgments

This work was supported by the National Research Foundation of Korea (NRF) grant funded by the Korea Government (MSIT) (No. 2022R1A2C4002583).

Supplementary Materials

Table S1: Summary of Laboratory Load Test Database. (*Supplementary Materials*)

References

[1] T. H. Bong, S. R. Kim, and B. I. Kim, "Prediction of ultimate bearing capacity of aggregate pier reinforced clay using multiple regression analysis and deep learning," *Applied Sciences*, vol. 10, no. 13, p. 4580, 2020.

[2] M. Etezad, A. M. Hanna, and T. Ayadat, "Bearing capacity of a group of stone columns in soft soil," *International Journal of Geomechanics*, vol. 15, no. 2, Article ID 04014043, 2015.

[3] A. W. Stuedlein and R. D. Holtz, "Bearing capacity of spread footings on aggregate pier reinforced clay," *Journal of Geotechnical and Geoenvironmental Engineering*, vol. 139, no. 1, pp. 49–58, 2013.

[4] M. Kitazume, *The Sand Compaction Pile Method*, Taylor & Francis, London, UK, 2005.

[5] M. Hasan and N. K. Samadhiya, "Experimental and numerical analysis of geosynthetic-reinforced floating granular piles in soft clays," *International Journal of Geosynthetics and Ground Engineering*, vol. 2, no. 3, p. 22, 2016.

[6] T. H. Bong, A. W. Stuedlein, B. I. Kim, and J. P. Martin, "Bearing capacity of spread footings on aggregate pier reinforced clay: updates and stress concentration," *Canadian Geotechnical Journal*, vol. 57, no. 5, pp. 717–727, 2020.

[7] J. Han, *Principles and Practice of Ground Improvement*, Wiley, Hoboken, NJ, USA, 2015.

[8] M. T. Suleiman and D. J. White, "Load transfer in rammed aggregate piers," *International Journal of Geomechanics*, vol. 6, no. 6, pp. 389–398, 2006.

[9] M. F. Randolph, "Design methods of pile groups and piled rafts," in *Proceedings of the 13th Int. Conf. on Soil Mechanics and Foundation Engineering*, pp. 61–82, New Delhi, India, January 1994.

[10] R. D. Barksdale and R. C. Bachus, *Design and Construction of Stone Columns*, Report No. FHWA/RD 83/026, Federal Highway Administration, Washington, DC, USA, 1983.

[11] H. Aboshi and N. Suematsu, "Sand compaction pile method state-of-the-art paper," in *Proceedings of the 3rd International Geotechnical Seminar on Soil Improvement Methods*.

[12] B. I. Kim and S. H. Lee, "Comparison of bearing capacity characteristics of sand and gravel compaction pile treated ground," *KSCE Journal of Civil Engineering*, vol. 9, no. 3, pp. 197–203, 2005.

[13] C. H. Trautmann and F. H. Kulhawy, "Uplift load-displacement behavior of spread foundations," *Journal of Geotechnical Engineering*, vol. 114, no. 2, pp. 168–184, 1988.

[14] E. E. Debeer, "Experimental determination of the shape factors and the bearing capacity factors of sand," *Géotechnique*, vol. 20, no. 4, pp. 387–411, 1970.

[15] J. L. Briaud and P. Jeanjean, "Load settlement curve method for spread footings on sand," in *Proceedings of the Settlement '94, Vertical and Horizontal Deformations of Foundations and Embankments*, pp. 1774–1804.

[16] J. M. Duncan and C. Y. Chang, "Nonlinear analysis of stress and strain in soils," *Journal of the Soil Mechanics and Foundations Division*, vol. 96, no. 5, pp. 1629–1653, 1970.

[17] A. B. Cerato, *Scale Effect of Shallow Foundation Bearing Capacity on Granular Material*, PhD Thesis, University of Massachusetts Amherst, MA, USA, 2005.

[18] F. K. Chin, "The seepage theory of primary and secondary consolidation," in *Proceedings of the 4th Southeast Asian Conference on Soil Engineering*, pp. 21–28.

[19] P. Sultana and A. K. Dey, "Estimation of ultimate bearing capacity of footings on soft clay from plate load test data considering variability," *Indian Geotechnical Journal*, vol. 49, no. 2, pp. 170–183, 2019.

[20] S. B. Tan, "Empirical method for estimating secondary and total settlement," in *Proceedings of the 4th Asian Regional Conference on Soil Mechanics and Foundation Engineering*, pp. 147–151.

[21] J. L. Briaud and R. Gibbens, "Predicted and measured behavior of five spread footings on sand," in *Proceedings of the a Prediction Symposium Sponsored by the Federal Highway Administration at the Occasion of the Settlement '94 ASCE Conference*, Texas, USA, 1994.

[22] A. J. Lutenegger and M. T. Adams, "Bearing capacity of footings on compacted sand," in *Proceedings of the 4th International Conference on Case Histories in Geotechnical Engineering*, St. Louis, Missouri, USA, 1998.

[23] D. A. Greenwood, "Mechanical improvement of soils below ground surface," in *Proceedings of the Ground Engineering Conference*, pp. 9–20, Institute of Civil Engineering, London, UK, 1970.

[24] J. M. O. Hughes, N. J. Withers, and D. A. Greenwood, "A field trial of the reinforcing effect of a stone column in soil," *Géotechnique*, vol. 25, no. 1, pp. 31–44, 1975.

[25] B. Jellali, M. Bouassida, and P. D. Buhan, "A homogenization method for estimating the bearing capacity of soils reinforced by columns," *International Journal for Numerical and Analytical Methods in Geomechanics*, vol. 29, no. 10, pp. 989–1004, 2005.

[26] A. S. Vesic, "Expansion of cavities in infinite soil mass," *Journal of the Soil Mechanics and Foundations Division*, vol. 98, no. 3, pp. 265–290, 1972.

[27] D. T. Bergado and F. L. Lam, "Full scale load test of granular piles with different densities and different proportions of gravel and sand on soft bangkok clay," *Soils and Foundations*, vol. 27, no. 1, pp. 86–93, 1987.

[28] J. K. Mitchell, "Soil improvement - state-of-the-art report," in *Proceedings of the 10th Soil Mechanics and Foundation Engineering*, vol. 12, pp. 506–565, International Society of Soil Mechanics and Foundation Engineering, London, UK.

[29] J. Brauns, "Initial bearing capacity of stone columns and sand piles," in *Proceedings of the Soil Reinforcing and Stabilizing Techniques in Engineering Practice*, pp. 497–512, New South Wales Institute of Technology, Sydney, Australia.

[30] H. T. V. Pham and D. J. White, "Support mechanisms of rammed aggregate piers. II: numerical analyses," *Journal of Geotechnical and Geoenvironmental Engineering*, vol. 133, no. 12, pp. 1512–1521, 2007.

[31] H. M. Algin and V. Gumus, "3D FE analysis on settlement of footing supported with rammed aggregate pier group," *International Journal of Geomechanics*, vol. 18, no. 8, Article ID 04018095, 2018.

[32] M. Das and A. Dey, "Prediction of bearing capacity of stone columns placed in soft clay using ANN model," *Geotechnical & Geological Engineering*, vol. 36, no. 3, pp. 1845–1861, 2018.

[33] M. Mohammadizadeh and M. Asadi, "Estimation of bearing capacity and settlement of spread footing over stone column reinforced clay using fuzzy models and artificial neural networks," *Indian Journal of Fundamental and Applied Life Science*, vol. 5, no. S2, pp. 3038–3050, 2015.

[34] S. Dadhich, J. K. Sharma, and M. Madhira, "Prediction of ultimate bearing capacity of aggregate pier reinforced clay using machine learning," *International Journal of Geosynthetics and Ground Engineering*, vol. 7, no. 2, p. 44, 2021.

[35] D. R. Helsel and R. M. Hirsch, *Statistical Methods in Water Resources*, USGS, TWRI-4-A3, Reston, VA, USA, 2002.

[36] J. M. Pitt, D. J. White, A. Gaul, and K. Hoevelcamp, *Highway Applications for Rammed Aggregate Piers in Iowa Soils*, Iowa DOT Project TR-443 Final Report, Ames, IA, USA, 2003.